DEPARTMENT OF THE INTERIOR
UNITED STATES GEOLOGICAL SURVEY

Prepared in Cooperation with the
JET PROPULSION LABORATORY, CALIFORNIA INSTITUTE OF TECHNOLOGY
FOR THE NATIONAL AERONAUTICS AND SPACE ADMINISTRATION

ATLAS OF MARS
1:5,000,000 GEOLOGIC SERIES
PHOENICIS LACUS QUADRANGLE
M SM-15/112 G, 1978
I-896 MC-17

NOTES ON BASE

This map sheet is one of a series covering the entire surface of Mars at nominal scales of 1:25,000,000 and 1:5,000,000 (Barton, 1973; Batson 1976). The major source of map data was the Mariner 9 television experiment (Masursky and others, 1970).

ADOPTED FIGURE

The figure of Mars used for the computation of the map projection is an oblate spheroid (flattening of 1/192) with an equatorial radius of 3393.4 km and a polar radius of 3375.7 km. This is not the height datum which is defined below under the heading "Contours".

PROJECTION

The Mercator projection is used for this sheet, with a scale of 1:5,000,000 at the equator and 1:4,336,000 at lat 30°. Longitudes increase to the west in accordance with usage of the International Astronomical Union (IAU, 1976). Latitudes are areographic (de Vaucouleurs and others, 1973).

CONTROL

Planimetric control is provided by photogrammetric triangulation using Mariner 9 pictures (Davies, 1973; Davies and Arthur, 1973) and the radio-tracked position of the spacecraft. The first meridian passes through the crater Airy-0 (lat 5.19° S) within the crater Airy. No simple statement is possible for the precision, but local consistency is 10-20 km.

MAPPING TECHNIQUE

A series of mosaics of Mercator projections of Mariner 9 pictures was assembled at 1:5,000,000.

Shaded relief was copied from the mosaics and portrayed with uniform illumination with the sun to the west. Many Mariner 9 pictures beyond those in the base mosaic were examined to improve the portrayal (Leventhal and others, 1973; Sharp and others, 1973; Sharp and Bridges, 1976). The shading is not generalized and may be interpreted with photographic reliability (Inge, 1972).

Shaded relief analysis and representation were made by Patricia M. Bridges.

CONTOURS

Since Mars has no seas and hence no sea level, the datum (the 0 km contour line) for altitudes is defined by a gravity field described by spherical harmonics through the fourth order and fourth degree. (Jordan and Lorell, 1973) combined with a 6.1 millibar atmospheric pressure surface derived from radiowo(ctation data (Kliore and others, 1973; Christensen 1975; Wu 1975).

The contour lines on most of the Mars maps (Wu, 1975) were compiled from Earth-based radar determinations (Downs and others, 1971; Pettengill and others, 1971) and measurements made by Mariner 9 instrumentation, including the ultraviolet spectrometer (Hord and others, 1974), infrared interferometer spectrometer (Conrath and others, 1973), and stereoscopic Mariner 9 television pictures (Blasius and others, 1973).

Formal analysis of the accuracy of topographic elevation information has not been made. The estimated vertical accuracy of each source of data indicates a probable error of 1-2 km.

NOMENCLATURE

All names on this sheet are approved by the International Astronomical Union (IAU, 1974-1975).

MC-17: Abbreviation for Mars Chart 17.
M SM -15/112 G: Abbreviation for Mars 1:5,000,000 series; center of sheet, 15° S latitude, 112° longitude; geologic map, G.

REFERENCES

Batson, R. M., 1973, Cartographic products from the Mariner 9 mission: Jour. Geophys. Research, v. 78, no. 20, p. 4424-4435.
_____1976, Cartography of Mars, 1975: The American Cartographer, v. 3, no. 1, p. 57-63.
Christensen, E. J., 1975, Martian topography derived from occultation, radar, spectral and optical measurements: Jour. Geophys. Research, v. 80, no. 20, p. 2909-2913.
Conrath, B. J., Curran, R. K., Hanel, R. A., Kunde, V. G., Maguire, W. W., Pearl, J. C., Pirraglia, J. A., Welker, J., and Burke, T. E., 1973, Atmospheric and surface properties of Mars obtained by infrared spectroscopy on Mariner 9: Jour. Geophys. Research, v. 78, no. 20, p. 4267-4278.
Davies, M. E., 1973, Mariner 9: Primary control net: Photogrammetric Eng., v. 39, no. 12, p. 1297-1302.
Davies, M. E., and Arthur, D. W. G., 1973, Martian surface coordinates: Jour. Geophys. Research, v. 78, no. 20, p. 4355-4398.
Downs, G. S., Goldstein, R. M., Green, R. R., and Morris, G. A., 1971, Mars radar observations—Preliminary report: Science, v. 174, no. 4016, p. 1324-1327.
Green, W. B., Jepsen, P. L., Kreznar, J. E., Ruiz, R. M., Schwartz, A. A., and Seidman, J. B., 1975, Removal of instrument signature from Mariner 9 television images of Mars: Applied Optics, v. 14, no. 1, p. 105-114.
Hord, C. W., Simmons, K. E., and McLaughlin, L. K., 1974, Mariner 9 ultraviolet spectrometer experiment: Pressure altitude measurements on Mars: Icarus, v. 21, no. 3, p. 292-302.
Inge, J. L., 1972, Principles of lunar illustration: Aeronaut. Chart and Inf. Center Ref. Pub., RP-72-1, 60 p.
Inge, J. L., and Bridges, P. M., 1976, Applied photointerpretation for airbrush cartography: Photogram. Eng., v. 42, no. 6, p. 749-760.
International Astronomical Union, Commission 16, 1971, Physical study of planets and satellites, *in* Proc. 15th General Assembly, 1970: Internat. Astron. Union Trans., v. XIVB, p. 128-135.
_____1974, Physical study of planets and satellites, *in* Proc. 15th General Assembly, 1973: Internat. Astron. Union Trans., v. XVB, p. 105-108.
_____1977, Physical study of planets and satellites, *in* Proc. 16 General Assembly, 1976: Internat. Astron. Union Trans. (in press).
Jordan, J. F., and Lorell, Jack, 1973, Mariner 9, an instrument of dynamical science: Presented at AAS/AIAA Astrodynamics Conf., Vail, Colo., July 16-18, 1973.
Kliore, A. J., Fjeldbo, Gunnar, Seidel, B. L., Sykes, M. J., and Woiceshyn, P. M. 1973, S-band radio occultation measurements of the atmosphere and topography of Mars with Mariner 9: Extended mission coverage of polar and intermediate latitudes: Jour. Geophys. Research, v. 78, no. 20, p. 4331-4351.
Leventhal, E. M., Green, W. B., Cutts, J. A., Jahelka, E. D., Johnson, R. A., Sander, J. J., Seidman, J. B., Young, A. T., and Soderblom, L. A., 1973, Mariner 9 image processing and products: Icarus, v. 18, no. 4, p. 75-101.
Masursky, Harold, Batson, R. M., Borgeson, W., Carr, M. H., McCauley, J. F., McEwen, C. A., Milton, D. J., Soderblom, L. A., Strobell, M. H., Wilhelms, D. E., Leighton, R. B., Sharp, R. V., Thompson, F. W., Briggs, G. A., Chandeysson, P. L. Shipley, E. N., Sagan, Carl, Pollack, J. B., Lederberg, Joshua, Leventhal, E. J., Hartmann, W. K., McCord, T. B., Smith, B. A., Davies, M. E., de Vaucouleurs, G. D., and Leovy, C. B., 1970, Television experiment for Mariner Mars 1971: Icarus, v. 12, no. 1, p. 10-45.
Pettengill, G. H., Rogers, A. E. E., and Shapiro, I. I., 1971, Martian craters and a warp as seen by radar: Science, v. 174, no. 4016, p. 1321-1324.
de Vaucouleurs, G., Davies, M. E., and Sturms, F. M., Jr., 1973, The Mariner 9 areographic coordinate system: Jour. Geophys. Research, v. 78, no. 20, p. 4395-4404.
Wu, S. S. C., Schafer, F. J., Nakata, G. M., Jordan, Raymond, and Blasius, D. R., 1973, Photogrammetric evaluation of Mariner 9 photography: Jour. Geophys. Research, v. 78, no. 20, p. 4405-4410.
Wu, S. S. C., 1975, Topographic mapping of Mars: U.S. Geol. Survey Interagency Report: Astrogeol. 63, 191 p.

Prepared on behalf of the Jet Propulsion Laboratory, California Institute of Technology under contract NSG-6122

CORRELATION OF MAP UNITS

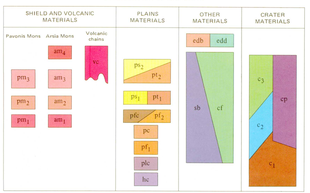

DESCRIPTION OF MAP UNITS

SHIELD AND VOLCANIC MATERIALS

pm$_3$ — PAVONIS MONS SHIELD MATERIAL–Forms upper flanks and summit of Pavonis Mons. Characterized by terraced linaments concentric to summit depression; cut by some radial and concentric lineaments. *Interpretation*: Volcanic flows of basaltic composition; youngest shield materials in region.

pm$_2$ — PAVONIS MONS FRACTURED SHIELD MATERIAL–Surrounds shield to the southwest; displays radial lineaments cut by radial linaments; slopes gently outward at about 2°. *Interpretation*: Lava flows of basaltic composition, possibly interbedded with volcanic tuff modified by wind erosion. Similar to units am$_2$ on this map and to Tharsis map (MC-9)

pm$_1$ — PAVONIS MONS AUREOLE MATERIAL–Forms northwest outer flank of Pavonis Mons directly north of this map area. *Interpretation*: Basal volcanic flow unit. Similar to unit am$_1$; may correlate with unit au on Tharsis map (MC-9)

am$_4$ — ARSIA MONS YOUNG SHIELD MATERIAL–Occurs in caldera and on north and south flanks of Arsia Mons. Caldera material flat and fracturedcc; flank material displays faint radial linaments. *Interpretation*: Fluid volcanic material; probably basaltic in composition, that filled caldera; also erupted and flowed down shield flanks from flank faults and vents. Lineaments probably are fractures.

am$_3$ — ARSIA MONS DOME MATERIAL–Forms flanks of Arsia Mons. Slopes of 4° to 6° display concentric radial and radial lineaments along which lines of craters occur. Similar to large shield mountains located in Tharsis map (MC-9) to north. Displays largest number of volcanic craters in map area. *Interpretation*: Viscous volcanic flows of more silicic composition such as basaltic andesite or andesitic basalt. Lines of craters probably are volcanic vents

am$_2$ — ARSIA MONS PITTED SHIELD MATERIAL–Forms terraced, lobate lower flanks of Arsia Mons. Slopes 1° to 2°. Pit lying southwest of dome cut by radial lineaments 50 to 150 km in length that trend northeast-southwest; pair lying northwest of dome displays rough pitted surface cut by radial lineaments trending northwest-southeast. *Interpretation*: Volcanic flows, possibly basaltic in composition, partially modified by wind erosion. May correlate with unit m on Tharsis map (MC-9)

am$_1$ — ARSIA MONS AUREOLE MATERIAL–Forms very gently sloping outer flanks of Arsia Mons. Displays mottled, faint lineaments radial to flanks of shield. *Interpretation*: Fluid volcanic flows, probably of basaltic composition, greatly modified by wind erosion; may correlate with unit au on Tharsis map (MC-9) to north.

vc — VOLCANIC CHAIN DEPOSITS–Occur as irregular to elongate deposits commonly within valleys or depressions; some linear features are characterized by chains of small rimless craters. Overlie or cut plains deposits. *Interpretation*: Volcanic material, possibly basaltic in composition, may be flows of low viscosity with included fragmental volcanic material, erupted from volcanic vents aligned along tectonic fractures. Relations indicate younger age than all volcanic plains

PLAINS MATERIALS

ps$_2$ — YOUNG SMOOTH PLAINS MATERIAL–Occurs in central part of map area, west of Claritas Fossae; cuts most smooth plains material in central part of Claritas Fossae. Nearly featureless except for thin, irregular cracks and very sparse, small, superposed craters. *Interpretation*: Lava flow, overlain by thick, young eolian deposits

ps$_1$ — THARSIS OLD SMOOTH PLAINS MATERIAL–Surrounds Arsia and Pavonis Montes. Occurs as dark, relatively smooth plain; distinct to indistinct lobate and radial lineaments visible at 1:4 million. *Interpretation*: Lava flows of basaltic composition, with fine grained eolian deposits that thin to south.

pl$_5$ — OLDER SMOOTH PLAINS MATERIAL–Occurs on Syria Planum; characterized by wide bright polygonal cracks, faint lineaments, and a few modified lobate impact craters. *Interpretation*: Lava flows marbled by thin eolian deposits

pl$_4$ — THARSIS OLD PLAINS MATERIAL–Occurs only in far western part of map. Forms dark smooth plain; indistinct lobate lineaments visible at 1:4m resolution. Small craters display vague light halos. *Interpretation*: Lava flows, possibly basaltic in composition, with indistinct lobe fronts and lava channels; mantled by thick eolian deposits

pl$_3$ — MODERATELY CRATERED PLAINS MATERIAL WITH FLOWS–Occurs in east-central and southcentral part of map area. Forms plains characterized by moderate crater populations and vague lobate lineaments; has fractures or streaks visible at high resolution. Very small craters commonly display distinct bright halos. Albedo moderately low. Radar spectra most sharply peaked of any unit on Mars. *Interpretation*: Unmantled or very thinly mantled volcanic flows of intermediate age; slight halos around superposed impact craters interpreted as fresh ejecta deposits

pl$_2$ — YOUNGER FRACTURED PLAINS MATERIAL–Occurs in Syria Planum and in southwestern corner of map area. Characterized by indistinct widely spaced lineaments 50 to 150 km in length that trend northwest-southeast near Noctis Labyrinthus and northeast-southwest in southeastern part of map area. Small craters in southwest part of map area display light "tails" and trend indistinct light halos. *Interpretation*: Volcanic flows and tuffs, possibly basaltic in composition, offset by faults

pl$_1$ — CRATERED PLAINS MATERIAL–Forms cratered plains in southern and eastern map areas. Surface appears relatively featureless except for numerous superposed small (8 km) craters and few indistinct lobate lineaments at 1:4m resolution. Higher resolution photograph shows knobby area and faint lineaments trending north. *Interpretation*: Thin lava flows, possibly basaltic in composition

pl$_0$ — OLD FRACTURED PLAINS MATERIAL–Occurs in central part of map area, at Claritas Fossae and north and south of Noctis Labyrinthus. Characterized by numerous subparallel or intersecting lineaments 100 to 200 km in length that trend north northwest-south southeast in eastern portion of Claritas Fossae and east-west in south southwest, and east northeast-west southwest in Noctis Labyrinthus. *Interpretation*: Volcanic flows and tuffs, possibly basaltic in composition; until fractured and fractured by tectonic forces

pc — CRATERED PLATEAU MATERIAL–Occurs on south-central part of area and at outliers to west; forms dark plains containing numerous degraded craters and numerous superposed craters. Closely spaced subparallel lineaments trend north northwest-south southeast. *Interpretation*: Ancient crustal material of basaltic or anorthositic composition. Interceptor plains may be lava flows cut or flooded impact craters

hc — HILLY CRATERED PLATEAU MATERIAL–Occurs in south-central part of area, east of unit plc; characterized by numerous degraded craters with flat or hummocky floors; some rims incompletely Widely spaced degraded lineaments trend east northeast-west southeast. *Interpretation*: Ancient crustal material, possibly mafitic or anorthositic in composition, faulted and degraded by eolian and mass-wasting processes

OTHER MATERIALS

edh — BRIGHT EOLIAN DEPOSITS–Occur as streaks or triangular "tails" extending in a southwesterly direction from small or medium-sized craters and as wide parallel streaks on smooth plains units. *Interpretation*: Eolian deposits

edd — DARK EOLIAN DEPOSITS–Occur as dark material surrounding old, degraded craters. *Interpretation*: Eolian deposits of fine-grained dark, possibly volcanic material deposited by wind. Some irregular dark areas may be rock outcrops of bright eolian deposits

sb — SLOPE AND BEDROCK MATERIAL–Occurs in northwest part of map area; forms slopes of steep, narrow, intersecting valleys in Noctis Labyrinthus area and broader valleys in western edge of Valles Marineris. Fogs of some slopes scalloped; others fresh and crisp. Some deposits of slumped material on gentler valley slopes. *Interpretation*: Exposed outcrops of underlying units and mass-wasted debris (talus or scree) derived from them

cf — CANYON FLOOR MATERIAL–Occurs as two patches of mantling material on floor of western end of Valles Marineris and small isolated patches on floors of some valleys in Noctis Labyrinthus. *Interpretation*: Depositional materials derived from mass wasting of canyon walls and (or) products of eolian deposition

CRATER MATERIALS

Craters form circular to near-circular areas depressed relative to their rims. They are classified according to their relative age by shape and morphology; craters <20 km in diameter not mapped. *Interpretation*: Impact craters

c$_3$ — CRATER YOUNGER THAN OR CONTEMPORANEOUS WITH SURFACE–Rim rough, raised above surrounding terrain; randomly distributed in unfractured plains and volcanic plains units; floors bowl shaped or flat

c$_2$ — PARTLY BURIED CRATER–Rim slightly raised above surrounding terrain; floors flat, commonly consist of same material as surrounding unit. Occur in older plains units and ancient crustal material

c$_1$ — EXHUMED CRATER–Rim smooth, commonly incomplete; floor flat or displaying mass-wasted material from rim; commonly cut by degraded lineaments

cp — CENTRAL PEAK MATERIAL–Occurs as rough, raised material in center of some c$_2$, c$_2$, and c$_3$ craters. *Interpretation*: Material uplifted by immediate rebound as result of impact

Contact–Queried where uncertain; dotted where ephemeral

Fault–Ball and bar on downthrown side

Narrow depression of graben

Lineament–Linear ridge or valley

Crater rim crest–May represent contact in places

Grooved or buried crater rim crest

Caldera rim

PHYSIOGRAPHIC SETTING

The Phoenicis Lacus quadrangle (named Lake of the Phoenix by Schiaparelli, 1877) includes some of the largest geologic features recognized on the terrestrial planets. Arsia and Pavonis Montes, ("South Spot" and "Middle Spot" of Mariner 9) rise 18 and 17 km, respectively, above the surrounding plateau to an elevation of about 27 km above the 6.1 millibar base level. These mountains and the two large volcanoes Ascraeus and Olympus Montes, located outside the quadrangle to the north, are also about 27 km in height; about three times as high as any volcano on Earth. The summit caldera of Arsia Mons, more than 100 km in diameter, is the largest known. Syria and Sinai Planu are part of the highest plateau on Mars, the Tharsis plateau; their relative elevation, 10 km, is twice that of the Tibetan Plateau, the highest plateau on Earth. Noctis Labyrinthus, the hub system of fault valleys at the west end of Valles Marineris which is located outside the quadrangle to the east, displays a more clearly developed pattern than any of the great fault valley systems on Earth, such as the East African rift valleys. The land slopes down to the northwest into Utopia Planitia (fig. 1); the difference in elevation between the volcanic peaks and the Amazonis low plains is greater than the relief from the top of the Andes to the bottom of the Peruvian trench. This great slope on Mars is similar to the continental shelf and slope that marks the transition between the continents and ocean basin floors on the Earth.

The lowest area in the quadrangle is 4 km above the 6.1 millibar datum; the lowest regions on Mars, Chryse Planitia northeast of the Tharsis Montes near the Viking 1 landing site, the bottoms of Hellas and Argyre Planitiae (basins) in the southern hemisphere, and the northern plains at about 65° N., are 3-4 km below datum.

MAPPING TECHNIQUES

The geologic map is plotted on a base map compiled from Mariner 9 photographs (see index map). Geologic mapping was done using low-resolution (1 km) A-frame photographs that were enhanced by the computer techniques in several versions of each picture were studied. High-resolution (100-meter) B-frame pictures, similarly enhanced, were used to aid in the interpretation and description of geologic units. The A-frame mosaic and map tell where units are; the B-frame pictures tell what they are. Information used to locate and define units includes radar observations in 1971, 1973, and 1975-76 and Mariner 9 occultation, infrared, ultraviolet, and television experiments (Masursky and others, 1970); stereopair stereoscopic photographs (Christensen, 1975; Wu, 1975), Goldstone and Arecibo radar spectra and reflectivity in the zenith angle range most useful for high (small) geologic units (fig. 2A; Simpson and others, 1977; Tyler and others, 1977).

The 27-km elevation of the summits of the mountains is based on stereoscopic photogrammetric determinations combined with UV and IR spectrometry and ground-based radar. Unfortunately, data from these three sets of data for Arsia and Pavonis Montes could not be reduced; the true elevations from a single datum are yet to be determined.

GEOLOGIC SUMMARY

Most of the rocks in the southern hemisphere of Mars are materials of ancient, heavily cratered terrain, whereas rocks in the northern hemisphere are composed primarily of younger lava flows that covered the ancient crustal material. The bimodality of terrain is expressed by a relative difference in elevation between the two hemispheres, the northern plains being as much as 2 km below Mars base level (6.1 mb), the southern highlands 3-4 km above it. Isostatic equilibrium between the two hemispheres (Phillips and Saunders, 1975) may have been reached when less dense crustal material under the northern flows was thinned by mantle-convection currents that eroded the underside of the crust and deposited the low-density material under the highlands to the south. A similar hypothesis was proposed for thickening of the Colorado Plateau, an isostatically compensated area that now stands high but was below sea level during most of its geologic history (Roy, 1968).

Although the Pavonis Lacus quadrangle lies south of the Martian equator, only a small area in the south-central part of the map area contains ancient crustal material. Most of the materials in the map area are volcanic flows similar to those in the northern hemisphere and young volcanic flows extruded contemporaneously with uplift of the Tharsis mountains and plateau, forming a great domical area.

The Syria-Sinai plateau is part of this great domical uplift, the apex of which lies in the Noctis Labyrinthus area (see also Masson, 1976). The presence of a large positive gravity anomaly in the plateau region (Phillips and Saunders, 1975) indicates that denser material must have been uplifted with the overlying low-density crustal rocks in the Tharsis area. However, it is not solely the result of isostatic uplift of a thickened section of low-density crustal material. Where ancient cratered terrain is exposed in the rocks in the apex of the dome (at the south end of Claritas Fossae), it is evident that the old Mars crust has been uplifted more than 8 km in that area. The uplift of Syria Planum is caused by a crustal portion of more intense magmatic activity like the "hotspot" described by Hartman (1970), or a "mantle plume" like that of the Morgan (1973). Convection currents initiated by the hotspot heat source may have thinned the crust and caused the uplift of the southern hemisphere. The northern hemisphere by dense mantle material and low-density crustal materials, by basaltic flows. The large shields of Arsia and Pavonis Montes and those of Ascraeus and Ascraeus Montes to the north may have formed over crustal fractures in the regional crustal hotspot.

The preservation of the Syria-Sinai uplift with its gravity anomaly indicates either that the area is held up dynamically or that the lithosphere is strong enough to prevent this distortion. The dome is only thinly mantled by volcanic flows and eolian deposits. The source for the gently sloping caprock lava flows on the dome is not apparent; the feeding fissures may now be buried by the younger flows. From the apex of the domical uplift, older and older mantling volcanic rocks are exposed to the east and west, like shingles on a roof. Beneath the mantle cratered terrain is completely exposed 2,500 km to the east and 2,000 km to the west.

Doming was accompanied by large-scale faulting to the north, south, and west of the Syria-Sinai dome. The fault valleys of Noctis Labyrinthus (fig. 2A) and Valles Marineris (fig. 2B), radiating faults also occur at greater distance to the Elysium, Memnonia, and Cerberus Fossae areas. Valles Marineris may be a giant rift or graben fault system and represent a complex large graben or rift formed as part of the uplift process. The intersecting fault pattern at Noctis Labyrinthus at the apex of the uplift resembles similar fault systems over salt domes in the gulf coast of the United States (Halbouty and Hardin, 1954) and experimentally produced faults over uplifts (Cloos and Cloos, 1934).

The great shields form two-or three-flated mountains. The shields of Arsia and Pavonis Montes show evidence of at least four episodes of volcanism; the gradation of the older shield units indicates that the recurrent extrusions that formed the volcanoes were separated by periods of intense wind erosion. The radiant extrusion, Arsia Mons aureole material (unit am$_1$), appears very degraded. The aureole around Olympus Mons also appears to be much more eroded; one explanation might be that it consists of early shield materials that correspond to Arsia Mons aureole material in this map area. Similar early widespread material also occurs at the foot of Ascraeus and Pavonis Montes, although it is not designated as a separate unit because it is too small to map. The younger lava flows (unit am$_2$), present at both Arsia and Pavonis Montes, may be absent or uncommon at Olympus Mons, was extruded; this unit is probably equivalent to the oldest shield in the Tharsis quadrangle. The shield materials that have been eroded into constructs were then extruded; they are equivalent to the sparsely cratered shield unit in the Tharsis map area. Finally, a young unit (unit am$_4$) formed the summit craters. It flows outward from the northern and southern flanks of Arsia Mons, and spread radially along the base of the volcano.

The allinement of the great volcanoes along the margin of the plateau may be analogous to the Andean volcanoes that occur along the margin of the South American plate on Earth or to Mount Hood, Mount Shasta, and Mount Rainier along the margin of the American plate in the Pacific northwest of the United States. However, the absence of other structural evidence of plate motion, such as magnetic stripes or a trench, makes the analogy with terrestrial plate tectonics not taking place or be, at most, incipient or minor in extent (Davie, 1963; Wilson, 1963; Masursky, 1973; Carr, 1976).

The common height (27 km) of Olympus Mons and the three large volcanoes along the margin of the plateau suggests that they are fed by a common, or at least similar, plumbing system. Elysium Mons and Hecates Tholus, in the Elysium volcanic field, are other features of nearly accordant, though lower, height (9 to 11 km). Structures of still lower, accordant elevation are seen in the continental volcanic centers of low relief around Hellas at Hadriaca and Amphitrites Paterae. These volcanoes, which are 1-2 km high, have a similar regional magma-feeder system, are common in terrestrial volcanic fields.

The composition of the rock units in the map area must be inferred from Earth and Moon analogues. The volcanic shield materials are probably basaltic or andesitic like the volcanoes in the Pacific northwest. Both the grain shield shape and the individual flow shapes suggest a basaltic composition. An exception is the uppermost flows on Arsia Mons, which, being shorter and thicker, may closely resemble andesitic basalt flows. The younger flank eruptions have flow shapes that resemble the basalt flows in Hawaiian volcanoes. The flows that produced the materials of extensive volcanic plains are inferred, from the lobate flow fronts visible in the high-resolution pictures, to be basaltic in composition, like lunar mare material. The composition of rocks exposed in the walls of Valles Marineris is less clear. Darker, more resistant layers may represent basaltic lava flows interlayered with lighter, less resistant pyroclastic deposits of more silicic composition, or eolian deposits. The ancient, heavily cratered crustal rocks may be anorthositic or mafitic in composition like the lunar highland rocks and some ancient terrestrial crustal rocks.

Many dark streaks are common and record the deposition and erosion of wind-blown materials during and after the 1971 planet-wide dust storm observed in Mariner 9 television pictures. Most streaks are bright, streaks of fine-grained eolian (loess) deposits, trend northwest-southeast on the smooth plain units. Bright tails extend southwest from craters in the southwestern corner of the map area. Dark tails trending west from small craters in the southern region may be dark eolian deposits or dark bedrock stripped of bright eolian deposits.

GEOLOGIC AND STRATIGRAPHIC HISTORY

The earliest episode of geologic history is represented by ancient, differentiated Martian crust that was extensively modified by the terminal phase of a heavy rain of impacting planetesimals (Hartmann, 1973; Soderblom and Wise, 1976) evidenced from the craters cover most of the ancient crust. Large areas of this ancient cratered terrain (hilly and cratered) are exposed in the southern hemisphere but occur only locally in the map area. The ancient terrain was fractured and extensively degraded by eolian and mass-wasting processes. Contemporaneous with and following the later stages of heavy cratering, the ancient crustal material was inundated by a succession of lava flows or impact debris, or both, to form the interceptor plains of the cratered plateau unit. Absolute ages for Martian rocks like those obtained for lunar samples by radiometric dating are not available, but estimates can be made (see below). Relative ages can be derived from geologic relations of overlap, intersection, and degradation. A rough estimate of relative age relations for units not in contact can be obtained from crater counts (Fig. 3, Table 1) using the technique described by Shoemaker and Morris (1972), Hartmann (1973), Soderblom and Lee (1974) and Blasius (1976). By this technique, crater densities determinations of 225 ± 75 for the hilly cratered plateau material and 125 ± 11 for the cratered plateau material, indicate that the hilly unit is older in the map area. Curves derived from crater counts of similar ancient crustal materials in other map areas (Meyer and Grolier, 1977; Schaber, 1977) indicate a relative age approaching that of the ancient lunar crustal material, 4 to 4.3 b.y. Ages for lunar materials are based on isotope ration obtained for returned lunar samples and lunar crater counts; from these two data sets Soderblom and his coworkers (1974) have constructed an integrated lunar flux curve (fig. 4). Since no samples have been returned from Mars, the Martian flux curve derived by them is based solely on Martian crater counts relative to lunar crater counts. Crater-density determinations for the two oldest units, when compared with the derived Martian flux curve, yield relative ages of approximately 3 and 1.5 b.y. The apparent age discrepancy between the crater curves and ages derived from crater-density determinations is probably produced primarily by the limitations of the lunar flux curve for ancient ages (fig. 4B) and secondarily by factors such as Neukum and Wise, 1976). Comparisons between Viking and Mariner 9 crater counts in other areas have shown that the higher resolution and discrimination of the Viking photographs yield crater densities that are higher by a factor of two or three for counts on Viking photographs. A new Viking flux curve, derived from Viking counts, will be constructed and probably will yield older relative ages for these units. Other factors that may have influenced the crater-density age determinations are: (1) the small area contained in this map is not a statistically valid sample; (2) the oldest rocks probably are resurfaced in this area; (3) ages from density determinations using the Soderblom technique based on craters in the 4 to 16-km-diameter range rather than crater curves that include the large old craters that characterize the ancient terrain give biased ages that are too young. The relative ages for the younger map units (fig. 4B) appear to be more reasonable; no true ages for Martian materials will be known until samples are returned from the Martian surface.

Some time later, basaltic flows inundated most of the northern hemisphere of Mars. Units similar to the northern volcanic flows covered part of this map area, lapping onto the ancient crustal material that forms the old fractured plains and cratered plains units. Crater density determinations of 85±9 and 80±9 for these units, respectively, yield estimated ages of slightly less than 3 billion years. However, the old fractured plains unit probably is somewhat older than the cratered plains unit; fracturing of the fractured plains unit that accompanied the beginning stages of uplift of the Tharsis Plateau may have destroyed some craters; as a result, age determinations could be deceptively young. The old fractured plains unit probably predates uplift; the cratered plains unit probably postdates or is contemporaneous to uplift. The cratered plains unit spreads widely in the low area around the uplift, and probably underlies the younger flows of the Tharsis plains units in the western part of the map area.

After a period of quiescence, renewed uplift in the Tharsis plateau was accompanied by extrusion of the Tharsis volcanic flows. Crater density determinations of 50±7 for the young fractured plains unit, 45 ± 7 for the old smooth plains unit, and 40±6 for the young smooth plains unit (fig. 4A) in this plain indicate that these units were extruded over a relatively short time period, about 500 m.y. ago. Crater flux curves for the young fractured plains and the old smooth plains unit are similar in the 4- to 10-km crater-diameter range, suggesting that the units are equivalent in age.

The last range of volcanic activity resulted in the construction of Pavonis Mons and Arsia Mons. These huge volcanic shields appear, from crater density determinations, to have been formed approximately 100 to 300 m.y. ago; 200 m.y. may be the lower limit of age determinations using count craters made from Mariner 9 photographs. On the flanks of the volcanic shields, lines of craters along possible faults were inferred to be volcanic and eliminated from impact-crater count (see also Hartmann, 1973; Soderblom and others, 1974, and Blasius, 1976). Most of the volcanic material that makes up the Tharsis plains and shield volcanoes appears to be basaltic in composition, shortly; stubbier flows near the summit of Arsia Mons may indicate a more silicic composition (andesitic basalt) for those flows.

The caldera-filling and flank flows that spread radially outward from the flank fissures revert to the shapes characteristic of basaltic flows; they display grooves that may be lava channels. These flows may be 100 to 200 m.y. old. The volcanic shields and plateau-mantling flows resemble the Columbia plateau basalts and volcanic cones, the most common volcanic material, probably basalts in composition, fills fissures in the Noctis Labyrinthus and other areas; craters are commonly along the fissures and probably served as vents for volcanic material.

Crater counts of the shield volcanoes are difficult to obtain because volcanic craters (aligned along faults) must be deleted from the data set. The impact crater counts subset indicates that the three great shield volcanoes may differ slightly in age, with Arsia Mons slightly older than the northern volcanoes. The basal materials (Arsia Mons aureole material, Pavonis Mons aureole material, and Olympus aureole material) are successively less exposed from south to north. Deeper burial of the shield by late flank eruptions or less extensive eruption of the basal units may have caused this relation. Higher resolution pictures may resolve the question.

The contact between lower area between Syria Planum and the volcanic shields of Arsia and Pavonis Montes is volcanic-unit overlain by eolian debris collected; the age of this unit, based on crater-density determinations, is approximately the same as that of Arsia Mons.

Finally, bright and dark material was deposited as crater tails and irregular patches, from the deposits of reworked eolian material were defined from the 1971 and earlier planet-wide dust storms. These features, being highly mobile, will probably be seen in later photography, as change.

The position of the Viking 1 landing site, indicated on figure 4A, is a preliminary determination based on crater counts from Viking photographs; it is included here to indicate the relative ages of the map units based on the lower resolution Mariner 9 data.

TECTONIC HISTORY

The earliest evidence of tectonism in the area is seen in the east-northeast trending, extensively degraded linations cutting the ancient crustal rocks that pretrade Mariner 9 photographs of the plateau lava. Following deposition of the old volcanic flow unit, the old fractured plains, the first great uplift of the Tharsis plateau resulted in widespread fracturing of that unit along northeast-northwest, northwest-southeast, east-west and north-south trends. Evidence for at least three periods of uplift and fracturing along these trends can be found in the complex overlapping relations among the faults and the varying degree of degradation of the fault scarps in the Claritas Fossae and Noctis Labyrinthus areas; the oldest fractures are widened and degraded and the youngest fractures are relatively sharp and show little modification (Masursky and others, 1970; Wu, 1973) over a long time period. The relative ages of faults based on intersection and degradation, are shown on the tectonic map (fig. 2B). Tectonism, as inferred mainly from the fracturing of the old fractured plains unit, caused the uplift of rose diagrams that show the varying direction and intensity of faulting. During this extensional period, the ancient crust in the map area were buried by successive outpourings of basaltic flows extruded from vents along established fractures that were created during the first period of uplift. These vents tapped magma chambers developed over possible hotspots in the mantle under the Tharsis plateau. Lava channels, flow lobes, and other features visible in the photographs suggest that vents along an inferred fault, whose northeast-southwest trend coincides with the location of Arsia, Pavonia, and Ascraeus Montes, were probably the surface outlets for most of the basaltic flows. After deposition of the Tharsis volcanic flow units, localized uplift of the central part of the area created the Noctis Labyrinthus, Claritas Fossae, and Syria-Sinai Plana areas to their present form. The extent and time of the old east-west fracture trends that accompanied uplift resulted in the formation of the large rift valleys that form Valles Marineris, chasms of the magnitude of the Grand Canyon. The Noctis, Claritas, and Cerberus Fossae in the Claritas Fossae area follow the east-west fracture trend. Renewal of the northwest-trending fractures in the Claritas Fossae area, which accompanied differential uplift in the south-central part of the map, shows this area above the surrounding terrains; the ridge that makes up the Claritas Fossae area is topographically displaced in a dextral transverse sense (fig. 2, Simpson, et al., 1977). The ancient crustal rocks were raised to their present elevation by similar faulting episodes and by the tectonism that formed the Claritas Fossae ridge. This great tilted fault block has a vertical displacement greater than 8 km; it is the largest tectonic feature on the planet. It resembles the great linear uplift east of Mare Smithii, which has a displacement of the crustal rocks of about 8 km. The east-facing hemisphere of the Moon shows down to the east such that the floor of Mare Smithii is 5 km below the mean lunar radius; the crest of the ridge forms the highlands east of Smithii. The Mare Smithii is more intensively faulted and its volcanic rocks are more highly developed.

The tectonism that formed the uplifted areas of Arsia and Pavonis Mons and the emplacement of young volcanic material along renewed north-south, northeast-southwest and northwest-southeast-trending fractures cut all basaltic flow units in the Tharsis region, the youngest in the map area formed by volcanism associated with tectonism.

ACKNOWLEDGEMENTS

The authors wish to thank Stanley E. Granato for his work on the preliminary version of the map and Joseph W. Boyce for his assistance with crater density determinations.

REFERENCES

Blasius, K. R., 1976, The record of impact cratering on the great volcanic shields of the Tharsis region of Mars: Icarus, v. 29, no. 3, p. 343-362.
Carr, M. H., 1975, Geologic map of the Tharsis region of Mars: U.S. Geol. Survey Inv. Ser. Map I-893 (MC-9).
Carr, M. H., 1976, The volcanoes of Mars: Sci. American, v. 234, no. 1, p. 32-43.
Christensen, E. J., 1975, Martian topography derived from occultation, radar, spectral and optical measurements: Jour. Geophys. Research, v. 80, no. 20, p. 2909-2913.
Cloos, Ernst and